

# ON A PROJECTION METHOD FOR THE NUMERICAL INTEGRATION OF CONSTITUTIVE EQUATIONS INVOLVING LARGE INELASTIC AND INCOMPRESSIBLE DEFORMATIONS

Marian Sielenkämper<sup>1</sup>, Jan Dittmann<sup>1</sup> and Stephan Wulfinghoff<sup>1</sup>

<sup>1</sup> CAU Kiel  
Kaiserstr. 2, 24143 Kiel, Germany  
{mfs,jd,swu}@tf.uni-kiel.de

**Key words:** Inelasticity, Finite Deformation Plasticity, Kinematic Hardening, Projection Method, Incompressibility Constraint

**Abstract.** Finite deformation plasticity often involves the multiplicative split of the deformation gradient into an elastic and plastic part. Motivated by observations in physics, the plastic part is assumed to be volume preserving, i.e., the plastic part of the deformation gradient is unimodular. In order to not accumulate errors, in the best case, one fulfills this constraint exactly to obtain accurate results (see, e.g., [3]). While other approaches were pursued as well, many authors therefore adopted the use of the exponential map, which is a geometric integrator preserving the plastic incompressibility. However, its computation is not straightforward and performing the eigenvalue decomposition and its linearization for the exponential function is numerically elaborate. Therefore, in this work, a new approach which also exactly preserves the incompressibility constraint is developed. It makes use of a projection of all symmetric tensors onto the manifold of unimodular tensors. The proposed method is compared to models utilizing the exponential map in numerical experiments.

## 1 INTRODUCTION

Nowadays in finite plasticity modeling, many models make use of the multiplicative split of the deformation gradient into an elastic and plastic part, which was introduced by [1, 2]. This split is depicted in Figure 1, where the initial configuration is deformed by the plastic deformation gradient  $F^P$ , yielding the intermediate configuration. Next, the intermediate configuration is deformed by the elastic deformation gradient  $F^e$ , yielding the current configuration. To incorporate kinematic hardening into the model, we employ a further split of  $F^P$ , which was pursued by [4] (see also [5]). Due to observations from physics, one assumes  $F^P$  to be unimodular, i.e.,  $\det(F^P) = 1$ . In many works, this is dealt with by using the exponential map as a geometric integrator, which exactly preserves the incompressibility of the plastic deformations (see, e.g., [6, 7, 5] among many others). In this work however, we employ a projection method which also intrinsically ensures the plastic incompressibility.

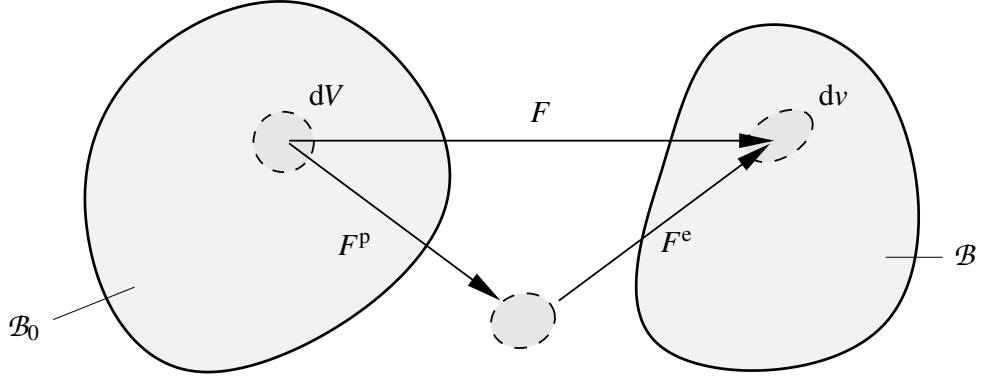


Figure 1: Multiplicative split of the deformation gradient. Reference configuration on the left, intermediate configuration at the bottom center and the current configuration on the right.

## 2 Theory of the model

### 2.1 Kinematics

As specified in the introduction, this model pursues the multiplicative split of the deformation gradient, i.e.,

$$F = F^e F^p. \quad (1)$$

This allows to introduce the left elastic and right inelastic Cauchy-Green tensors

$$b^e = F^e F^{eT}, \quad C^p = F^{pT} F^p. \quad (2)$$

Further, in analogy to [4], we split the plastic deformation gradient as follows

$$F^p = F^{pe} F^{pd}. \quad (3)$$

Here,  $F^{pe}$  is the energetic part and  $F^{pd}$  is the dissipative part of  $F^p$ . This definition allows to define a dissipative stretch  $C^{pd}$  as

$$C^{pd} = F^{pdT} F^{pd}. \quad (4)$$

Additionally, the Kirchhoff stress tensor

$$\tau = J\sigma = F^e S^e F^{eT} \quad (5)$$

can be given in terms of the Cauchy stress  $\sigma$  and the Jacobi determinant  $J$  or the second Piola-Kirchhoff stress tensor  $S^e$ . Finally, we can define  $b^{pe}$  as the plastic energetic left Cauchy-Green tensor defined via

$$b^{pe} = F^{pe} F^{peT}. \quad (6)$$

### 2.2 Contributions to the Helmholtz free energy

For the elastic contribution, a Neo-Hookean elastic energy is assumed in the form of

$$\psi_e(b^e) = \frac{\lambda}{4} (J^{e2} - 1 - 2\ln(J^e)) + \frac{\mu}{2} (I_{b^e} - 3 - 2\ln(J^e)) \quad (7)$$

where  $I_{b^e}$  denotes the first invariant of  $b^e$ ,  $J = \det(F)$  and  $\lambda$  and  $\mu$  are Lamé parameters. Further, for the isotropic hardening, we assume a Voce-type hardening in the form of

$$\psi_h = H \left( \alpha + \frac{\exp(-\beta\alpha)}{\beta} \right), \quad (8)$$

where  $H$  and  $\beta$  are material parameters and  $\alpha$  is the equivalent plastic strain. The kinematic hardening energy  $\psi_k$  is taken to be

$$\psi_k = \mu^p C^p : C^{pd-1}, \quad (9)$$

where  $\mu_p$  is a material constant. The dissipation potential is taken to be

$$\phi = \begin{cases} \sqrt{\frac{2}{3}} \sigma_{y0} \|D^p\|; & \text{if } \text{tr}(D^p) = 0 \\ \infty; & \text{else,} \end{cases} \quad (10)$$

where  $D^p$  is the symmetric part of the plastic velocity gradient and  $\sigma_{y0}$  is the initial yield stress. Next, the flow rule and yield criterion read

$$D^p = \gamma \frac{\partial f}{\partial \Sigma^e}, \quad (11)$$

and

$$f = \|(\Sigma^e - \Sigma^b)'\| - \sqrt{\frac{2}{3}}(\sigma_{y0} + q) \leq 0. \quad (12)$$

Here,  $\Sigma^e$  is the Mandel stress w.r.t. the intermediate configuration and  $\Sigma^b$  is the Mandel back stress defined via

$$\Sigma^e = C^e S^e, \quad \Sigma^b = 2F^{peT} \frac{\partial \psi_k}{\partial b^{pe}} F^{pe}. \quad (13)$$

With all the energetic contributions defined, the full rate potential reads

$$\pi = \psi_e(b^e) + \psi_h(\alpha) + \phi + \mu^p C^{pd-1} : \dot{C}^p. \quad (14)$$

### 2.3 Treatment of the incompressibility constraint

In finite strain plasticity, it is important to fulfill the plastic incompressibility with high accuracy to not accumulate errors (see, e.g., [3]). Therefore, we introduce an unconstrained counterpart  $\hat{C}^p$  to  $C^p$  such that

$$C^p = (\det(\hat{C}^p))^{-\frac{1}{3}} \hat{C}^p. \quad (15)$$

Here,  $\hat{C}^p$  is a positive definite symmetric but otherwise arbitrary tensor. This intrinsically ensures the unimodularity of  $C^p$  by only taking the unimodular part of  $\hat{C}^p$ , which is depicted in Fig.2. In analogy, a reparametrization for  $C^{pd}$  is introduced as

$$C^{pd} = (\det(\hat{C}^{pd}))^{-\frac{1}{3}} \hat{C}^{pd}. \quad (16)$$

Further, a Frederick-Armstrong type hardening law is assumed. Therefore,  $C^{pd}$  is dependent on the plastic multiplier  $\gamma$  via

$$\hat{C}^{pd} = C_n^{pd} + 2\Delta\gamma \frac{b}{c} \Sigma_n^{b'}. \quad (17)$$

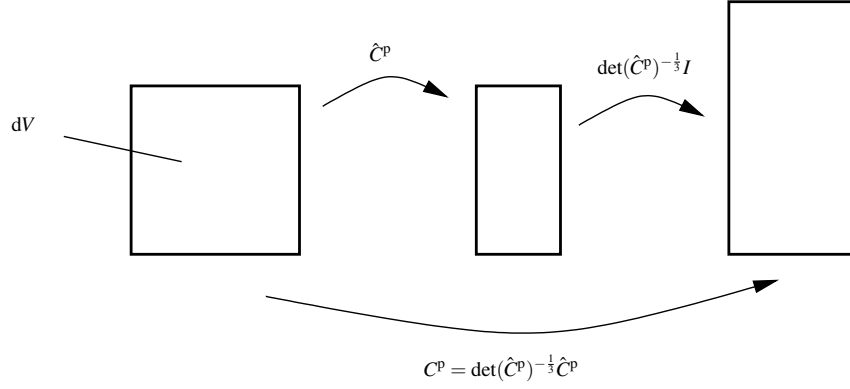


Figure 2: Reference volume on the left gets stretched by  $\hat{C}^p$ . Thereafter, it is volumetrically stretched back to its original volume by  $\det(\hat{C}^p)^{-\frac{1}{3}}I$ , rendering  $C^p$  unimodular.

## 2.4 Algorithmic counterpart to $\phi$

To minimize the potential from Eq. 14, we need to find an algorithmic counterpart  $\phi_\Delta$ , which is time-discrete and  $\phi_\Delta/\Delta t$  converges towards  $\phi$  with  $\Delta t \rightarrow 0$ . A possible choice is

$$\phi_\Delta = \begin{cases} \frac{1}{2} \sqrt{\frac{2}{3}} \sigma_{y0} \|c^p - I\| & ; \text{if } \det(c^p) = 1 \\ \infty & ; \text{else} \end{cases}. \quad (18)$$

Here,  $c^p$  can be interpreted as the plastic push-forward of  $C^p$  and is defined as

$$c^p = F_n^{p-T} C^p F_n^{p-1}. \quad (19)$$

## 2.5 Differentiability at $\Delta C^p = 0$

When trying to minimize the potential using a Newton scheme, one needs to differentiate it with respect to the internal variables. However, in its current form, it is not differentiable at  $\Delta C^p = 0$ , which complicates the numeric solution. Therefore, a further reparametrization is introduced as

$$\hat{C}^p = I + 2\Delta\gamma N^p. \quad (20)$$

Here,  $N^p$  is a symmetric tensor with the constraints  $\|N^p\| = 1$  and  $\Delta\gamma \geq 0$ . Now, it can be easily verified that the potential is differentiable at  $\Delta C^p = 0$ .

### 2.5.1 Removing the constraint $\|N^p\| = 1$

The goal when introducing the projection was to drop the incompressibility constraint. However, through removing it, we added the further constraint  $\|N^p\| = 1$ . To finally remove all constraint from the minimization problem, we introduce one last reparametrization

$$N^p = \frac{\tilde{N}^p}{\|\tilde{N}^p\|}. \quad (21)$$

Here,  $\tilde{N}^p$  is a symmetric, but otherwise arbitrary tensor. Obviously, the constraint is now gone.

### 2.5.2 Preventing singularities

As the observant reader might have already noticed, through reparametrizing the potential became invariant w.r.t. change in  $\det(\hat{C}^p)$  and  $\|\tilde{N}^p\|$ . For  $\det(\hat{C}^p)$ , this is depicted in Figure 3. Here, it is clear

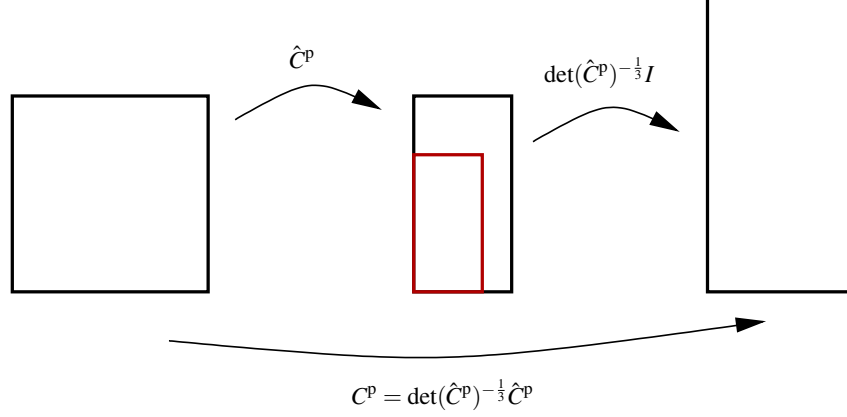


Figure 3: Changing the volumetric part of  $\hat{C}^p$  does not change the resulting  $C^p$ .

that changing the volumetric part of  $\hat{C}^p$  does not induce any changes in the resulting  $C^p$ . Likewise, this is the case for  $\|\tilde{N}^p\|$ , which renders the system matrix  $\partial^2\pi/\partial z^2$  singular. Here,  $z$  is the vector of internal variables. To overcome this singularity, an artificial regularization energy  $\pi_R$  is introduced as

$$\pi_R = \frac{1}{2}A((\hat{\text{III}}^p - 1)^2 + (\|\tilde{N}^p\| - 1)^2). \quad (22)$$

This term may be interpreted as a spring with spring constant  $A$  pulling  $\hat{\text{III}}^p$  and  $\|\tilde{N}^p\|$  towards 1. Here, it has to be noted that choosing  $A$  is arbitrary, since it won't have an influence on the final solution. This is due to the fact, that since the potential is, apart from the regularization energy, free of  $\hat{\text{III}}^p$  and  $\|\tilde{N}^p\|$ . Therefore, the regularization energy is always 0 at the minimum. Further, this means that while  $\pi_R$  allows us to find the solution by removing the singularity, it has no influence on the final solution. Now, in the results section, we minimize the potential

$$\Pi = \int_{\mathcal{B}} (\psi_e + \psi_h + \tilde{\psi}_k + \phi_\Delta + \pi_R) dV. \quad (23)$$

## 3 Results

To verify the results of the presented algorithm, they are compared to a necking of a circular bar example from [6]. The distribution of the equivalent plastic strains for the deformed bar are shown in Fig. 4. Additionally, the material parameters used in the finite element model are given in Tab. 1. Further, the convergence of the proposed method was analyzed with respect to the amount of time steps. Therefore, the necking displacement is plotted against the elongation in Fig. 5. Here, one can see the solution is converging against roughly 3.75mm. For already 30 time steps, it is fairly close to the converged solution. Additionally, the resulting necking displacements are very close to the ones from [6].

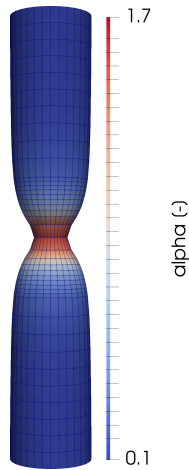


Figure 4: Distribution of the equivalent plastic strain  $\alpha$  over the deformed bar after loading.

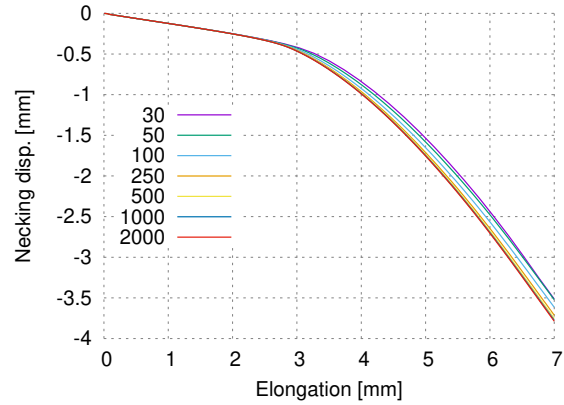


Figure 5: Convergence of the necking displacement vs. Elongation for varying amount of time steps.

| $\kappa$ [MPa] | $\mu$ [MPa] | $\sigma_{y0}$ [MPa] | $\sigma_{y\infty}$ [MPa] | $\beta$ | $H$ [MPa] |
|----------------|-------------|---------------------|--------------------------|---------|-----------|
| 164210         | 80193.8     | 450                 | 715                      | 16.93   | 129.24    |

Table 1: Material constants for necking of a circular bar.

#### 4 Summary and Outlook

In this paper, a new model to overcome incompressibility constraints in finite deformation mechanics was proposed. The model uses a projection which projects an unconstrained counterpart to  $C^p$  onto the manifold of unimodular tensors to exactly satisfy the constraint. Finally, the model was verified using an example from the literature. Here, the results showed to be very promising. Therefore, in the future, further materials with incompressibility constrained, e.g., shape memory alloys or rubbers, may be modeled using this projection method.

#### Acknowledgments

Financial support of subproject A3 *Cooperative Actuator Systems for Nanomechanics and Nanophotonics: Coupled Simulation* of the Priority Programme SPP 2206 by the German Research Foundation (DFG) is gratefully acknowledged by M.S. and S.W.. Funding by the German Research Foundation (DFG) for the project P12 within the framework of the research training group GRK 2154 “Materials for Brain” is gratefully acknowledged by S. W. and J. D..

#### REFERENCES

- [1] Kröner, E. *Allgemeine Kontinuumstheorie der Versetzungen und Eigenspannungen*. Archive for Rational Mechanics and Analysis, Vol. 4, (1959).
- [2] Lee, E. *Elastic-plastic deformation at finite strains*. (1969).
- [3] Shutov, A.V. and Kreißig, R. *Geometric integrators for multiplicative viscoplasticity: analysis of*

- error accumulation*. Computer Methods in Applied Mechanics and Engineering (2010) **199**:700–711.
- [4] Lion, A. *Constitutive modelling in finite thermoviscoplasticity: a physical approach based on non-linear rheological models*. International Journal of Plasticity (2000):**16**:469–494.
- [5] Dettmer, W. and Reese, S. *On the theoretical and numerical modelling of Armstrong–Frederick kinematic hardening in the finite strain regime*. Computer Methods in Applied Mechanics and Engineering (2004) **193**:87–116.
- [6] Simo, J.C. *Algorithms for static and dynamic multiplicative plasticity that preserve the classical return mapping schemes of the infinitesimal theory*. Computer Methods in Applied Mechanics and Engineering (1992) **99**:61–112.
- [7] Miehe, C. *Exponential map algorithm for stress updates in anisotropic multiplicative elastoplasticity for single crystals*. International Journal for Numerical Methods in Engineering (1996) **39**:3367–3390.
- [8] Ortiz, M. and Stainier, L. *The variational formulation of viscoplastic constitutive updates*. Computer Methods in Applied Mechanics and Engineering (1999) **171**:419–444.